Paper No.
4479

CORROSION 2014
Collaborate. Educate. Innovate. Mitigate.
March 9-13, 2014 • Henry B. Gonzalez Convention Center • San Antonio, Texas, U.S.A.

Temperature Effects on a Galvanic Anode-Steel in Concrete System

M. Dugarte*, A.A. Sagüés**
* Department of Civil and Environmental Engineering, Universidad del Norte, Km. 5 Vía Puerto Colombia, Barranquilla, Colombia.
** Department of Civil and Environmental Engineering, University of South Florida, 4202 East Fowler Ave., Tampa, FL 33620, U.S.A.

ABSTRACT

Temperature changes affect current delivery and electrochemical assessment of galvanic anode - steel in concrete systems. Interfacial corrosion processes are thermally activated and hence temperature dependent. In addition, concrete resistivity varies with temperature with consequent change in any resistive polarization component that may be present. The present work explores temperature correction procedures. Galvanic current, electrode potentials and resistivity measurements were determined as a function of concrete temperature in outdoors reinforced concrete slabs where sacrificial point anodes were connected to the steel. Measured values were successfully standardized to an equivalent resistivity/current at a predefined reference temperature, through the application of a master temperature correction equation based on a differential formulation that derived correction parameters from short term fluctuations and filtered long term aging trends. A more refined steel cathodic polarization characterization was introduced and demonstrated by accounting for the effect of electrode potential, as an added term to the nominal activation energy of the cathodic reaction.

Key Words: temperature, concrete, corrosion, resistivity, activation energy.

INTRODUCTION

It is known that concrete temperature has a significant effect on cathodic and anodic current measurements performed in concrete structures. [1-4] Electrical resistivity of concrete is considerably affected by temperature as well and this phenomenon is further complicated by the changes in the pore water chemical composition that occurs along with the change in temperature.[4] However, with a growing but still limited number of exceptions the effect of temperature in the process of concrete reinforcement corrosion has not yet been extensively investigated. [4-11] In particular, it is of interest to have validated means of correcting galvanic

protection/prevention systems data obtained at various temperatures to the value that would be prevalent at a given standardized temperature. To increase the overall documented base of knowledge on this issue, results obtained for a galvanic anode–steel in concrete system are presented here. The aim of this work was to investigate the temperature dependence of the anodic and cathodic components in a galvanic system, especially based on the system response itself without depending on generic parameters adapted from the literature. It was desired also to determine appropriate corrections formulated in terms of an activation energy approach applied to concrete resistivity, anodic and cathodic currents, including an attempt to consider the value of the potential measurements in the latter.

Investigations of galvanic systems often seek to determine aging trends that affect the anode, as well as to determine the polarization characteristics of the reinforcing steel/concrete interface. For a system in the field, diurnal and seasonal temperature changes obscure the anode aging and steel cathodic polarization trends. However, the development of accurate temperature correction algorithms based on the behavior of the system itself is complicated, because aging, polarization and temperature changes occur simultaneously.

In this paper a differential approach is used whereby the response of the system to short term changes in temperature (during which anode aging is assumed to have been negligible) is used to glean the effect of only temperature changes. Especial attention is given to the determination of cathodic behavior of the steel, but temperature corrections for the anode current and the concrete resistivity are addressed too.

SYSTEM EXAMINED AND EXPERIMENTAL PROCEDURE

This work was conducted concurrent with a recent investigation on the behavior of galvanic point anodes for corrosion control in patch repairs. [12, 13] Six reinforced concrete slabs under ambient exposure conditions were evaluated to assess the temperature dependence of electrochemical measurements in the system. Each slab with dimensions 120 x 45 x 15 cm contained 12 embedded reinforcement bars # 7 (diameter ~ 22 mm) spaced every 10 cm. The six concrete specimens were cast from concrete with and without mixed-in chlorides as detailed elsewhere. [12]

Sacrificial point anodes were connected to the reinforcing steel simulating a typical repair installation as shown in Figure 1. Two types of anodes were installed in triplicate (3 slabs each type) with the following dimensions: Anode type C: diameter: 63 mm, thickness: 27 mm, zinc anode mass: 103 g. Anode type W: dimensions: 77 mm x 60 mm, thickness: 33 mm, zinc anode mass: 48 g. For the experiments reported here only one anode (the leftmost in Figure 1) was used in each slab; the anode was connected to rebars 1-5 and 10-12 which were all interconnected and residing in nearly chloride-free concrete, as the investigation was determining the ability of the anodes to provide cathodic prevention polarization to passive steel. The rest of the anodes and rebars were each disconnected and left at their respective open circuit conditions. The shaded portion near the center contained admixed sodium chloride to obtain 5.9 Kg/m^3 chloride ion (10 pcy). The test slabs were maintained outdoors (~ 20 km inland from Tampa Bay, FL) under normal ambient exposure. Further details are presented elsewhere. [12, 13]

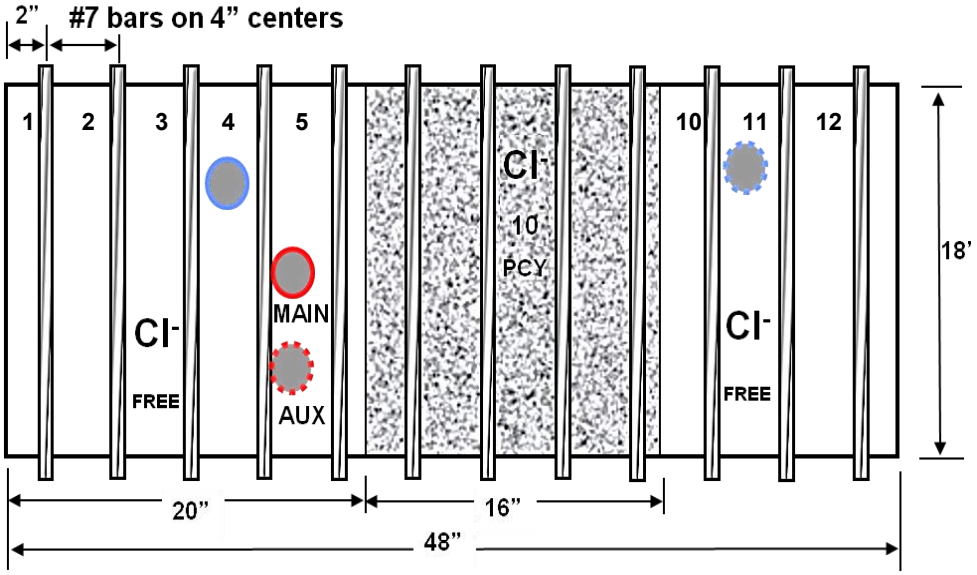

Figure 1: Yard Slab Test Configuration. Circles indicate embedded anodes. Rebars are numbered as indicated. For this investigation the only anode connected was that between rebars #3 and #4.

Experimental data for a temperature range from ~5 to 35ºC and over a 570 day period included concrete resistivity, individual rebar cathodic currents, anode current, and instant-off potential measurements (against internal embedded metal-metal oxide electrodes placed one each in the proximity of each rebar, and periodically calibrated against an external Copper-Copper Sulfate electrode (CSE)) of each rebar and the anode. All steel and anode potentials are reported in the CSE scale. A Nilsson model 400 Soil resistivity meter was used in a 4-point configuration to measure the concrete resistance as a function of distance along the main axis of the slab using procedure described elsewhere.[12] Other than for special geometry corrections for the end rebar cases,[12] the resulting resistance for each measurement was multiplied by a cell factor (68.6 cm, equal to the cross sectional area of the slab divided by the center-to-center rebar distance) to obtain the concrete resistivity for the concrete slice between each the pair of rebars. The resistivity of the chloride-free concrete is reported as the average of that obtained for rebar pairs 1-2, 2-3, and 11-12; the resistivity of the concrete in the chloride-containing region is reported as the average for rebar pairs 5-6, 7-8 and 8-9 (averages were obtained as the inverse of the average of the corresponding conductances).

The measured values of individual cathodic and overall galvanic anodic currents, as well as potentials and concrete resistivity, showed appreciable day to day and seasonal fluctuations that correlated well with variations in temperature. Those fluctuations obscured long term trends due solely to anode aging and other system evolution, and added scatter to determinations of anode performance. Consequently, the data were analyzed to extract parameters that could serve to approximately compensate for the temperature variation effects and reveal the anode aging and steel polarization trends of interest. Correction strategies are presented in the next section.

TEMPERATURE CORRECTION APPROACHES

Temperature Correction of Cathodic Current Density Measurements

The effect of temperature on electrochemical reactions is complicated by the mutual interaction between several reaction rate determining variables. [5] A simplified absolute reaction rate kinetics approach was used (see for example Kaesche [14] and observations by Tanaka [15]) where the cathodic rebar current density i_c was corrected for temperature, tentatively taking into account the potential E as well. The cathodic reaction on the steel rebars was considered to be oxygen reduction, which for much of the potential range of interest was found to proceed mainly under simple activation polarization. [13, 16] The basic ruling equation under those premises is Equation (1)

$$i_c = i_0 \times e^{-\frac{[Q_C - nF(1-\alpha)(E^O - E)]}{RT}} \quad (1)$$

Where n is the number of electrons involved in the reaction, and i_0 is an effective exchange current density for a hypothetical reference condition at potential E^0 where there is zero absolute potential difference between electrode and the solution, so at that potential thermal dependence is determined by a fixed ideal thermal activation energy Q_C. [15] In this tentative treatment the transfer coefficient α, i_0 and E^0 and Q_C were all assumed to be sufficiently weakly independent of temperature to be considered as constants within the temperature range of interest.[14] Per the form of Equation (1) at potentials other than E_0 the temperature dependence behaves, with E kept constant, as if an apparent activation energy $Q_C^* = [Q_C - nF(1-\alpha)(E^0 - E)]$, different from Q_C and influenced by the choice of reference electrode, would be in effect. [15] Alternatively, defining Equation (2), (3), and (4)

$$P = nF(1-\alpha) \quad \text{and} \quad Q_C{}' = Q_C - PE^o \quad (2)$$

$$i_c = i_0 \times e^{-\left[\frac{Q_C}{RT}\right]} \times e^{\left[\frac{P(E^O - E)}{RT}\right]} \quad (3)$$

$$i_c = i_0 \times e^{-\left[\frac{Q_C'}{RT}\right]} \times e^{-\left[\frac{PE}{RT}\right]} \quad (4)$$

Applying logarithms to Equation (4) (normalizing i to appropriate units) and differentiating to quantify the effect of changes in temperature and potential, Equation (5), (6), and (7) were obtained as:

$$lni_c = lni_0 - \left[\frac{Q_C'}{RT}\right] - \left[\frac{PE}{RT}\right] \quad (5)$$

$$\frac{\partial lni_c}{\partial E} = -\frac{P}{RT} \quad ; \frac{\partial lni_c}{\partial\left(\frac{1}{T}\right)} = -\frac{Q_C{}'}{R} - \frac{PE}{R} = \frac{-(Q_C{}' + PE)}{R} \quad (6)$$

$$R\ dlni_c = -\frac{P\ dE}{T} - (Q_C{}' + PE)d\left(\frac{1}{T}\right) \quad (7)$$

It should be noted that this approach assumes that the cathodic reaction is dominant at the potentials of interest, and neglects for simplicity the complicating effect of any anodic reaction (such as passive iron dissolution, or any incipient active corrosion) that may be taking place simultaneously on the rebar surface. Analysis of results was limited to only those rebars, far enough from the chloride laden zone, which did not show any signs of incipient activation during the test period. No special treatment was made however for the part of the polarization curve near the passive open circuit potential, where passive anodic dissolution introduce added complexity. Any influence of temperature on the reference electrode potential was likewise not considered.

The differential forms indicated above were used together with a set of rebar current densities i_{cj} (T_j, E_j) recorded at measured temperature T_j (K) and E_j (V), obtained at relatively short term (days) but irregularly spaced times t_j, to obtain the best fit values of Q_C' and P for the set. The fit was made by implementing Equation 7 in an approximate finite difference form, using guess global values of Q_C' and P, to obtain proposed values of $(R\ \Delta\ lni)_j$ for each time interval t_{j+1}- t_j. The proposed values were then subtracted from the actual $R\ \Delta\ lni_j$ value for each measurement interval, and the output values of Q_C' and P were those that minimized the sum of the differences squared. Using those parameters, the recorded current density data set was converted into the set that would have been measured if T were constant and equal to a reference temperature T_r using Equation (8):

$$i_j\ (T_r, Ej) = i_j\ \left(T_j, E_j\right) \times e^{-\frac{\left[Q_C{}' + PE_j\right]}{R}\left(\frac{1}{T_r} - \frac{1}{T_j}\right)} \quad (8)$$

Where T_r is the temperature for which all measurements are to be reported (chosen to be 25°C (298°K)).

Temperature Correction of Galvanic Current Measurements

Galvanic current is affected by the combined action of anode aging and attending temperature dependence of anode polarization, steel polarization, and of the resistivity of the concrete mediating both end of the galvanic macrocell. Given this complexity, noted in detail by others in connection with macrocell currents in concrete [4] a simplified empirical approach was used where the overall behavior of the anode current I_j in a data set similarly organized as that in the previous section, was assumed to follow an Arrhenius relationship with a constant apparent activation energy Q_A that when expressed in differential terms becomes Equation (9): [4- 6, 9-11]

$$\mathrm{I}_j\ (T_r) = \mathrm{I}_j\ \left(T_j\right) \times e^{-\frac{[Q_A]}{R}\left(\frac{1}{T_r} - \frac{1}{T_j}\right)} \quad (9)$$

with T_r = 298°K.

The value of Q_A was obtained from the best fit slope of a modified Arrhenius plot of the current-temperature data for each anode type. The modification, comparable to that described in the previous section, consisted of plotting the value R Δ(ln I) as function of Δ (T^{-1}), where the differences (Δ) are the change in measurement results for each slab of a given type of anode from the previous test date. The slope of the straight line best fitting the combined results for that anode was reported as the average apparent activation energy. This approach emphasizes the changes due to temperature variations, which are relatively short-term, and minimizes error in estimating Q_A introduced otherwise by the longer-term changes due mainly to anode and concrete aging and not related to temperature.[4, 5]

The temperature compensation described above for the anode current is only a rough approximation that ignores the complex interaction of the combined electrochemical processes at the anode and the rebar assembly, plus the effect of variation of electrolyte resistance with temperature. For example, unlike the treatment in the previous section, the correction did not take into account the value of the anode potential at the time the current was measured.

Temperature Correction of Concrete Resistivity

The resistivity of the concrete is a key factor affecting the corrosion process of reinforcing steel in concrete. [1, 12] It is well known that in general, the electrical resistivity of concrete increases with decreasing concrete temperature. In the short term, while the concrete pore network remains at a comparable degree of interconnectivity and water content, the relationship between the concrete resistivity and temperature is mainly due to changes in the conductivity of the pore water. It behaves comparably to similar alkaline solutions with ionic content typically in the order of 0.1 to 1 M following a generally Arrhenius-type dependence in temperature. [7-9, 17, 19-20] A procedure similar to that used for the anodic current temperature correction was employed here to obtain an apparent activation energy for the concrete resistivity. In this case, the temperature dependence on the concrete resistivity can be written as Equation (10):

$$\rho_j\,(T_r) = \rho_j\,\left(T_j\right) \times e^{-\frac{[Q_R]}{R}\left(\frac{1}{T_r}-\frac{1}{T_j}\right)} \qquad (10)$$

Where ρ_j (Ω.cm) is the concrete resistivity measured at T_j, T_j (K) is temperature, and Q_R (kJ/mole) is the apparent activation energy of resistivity. The differential formulation used in the other cases was employed here as well, providing a degree of compensation for the effects of long term system evolution.

RESULTS

Cathodic Current Corrections

Only data for rebars #1-3 and #11-12 in all slabs were processed for cathodic polarization characterization, as rebars #4-5 and #10 in some of the slabs had begun to show minor signs of active behavior later in the exposure period. In addition, data for rebar #11 in slab #4 after day 336 were not used as some incipient anodic action took place there as well. Figure 2 illustrates an example of the combined temperature and cathodic current data for three reinforcement bars in Slab 1 showing that the temperature has a strong effect on the cathodic current measurements. Values of Q_C' and P were obtained for each slab using the procedure listed

above and summarized in Table 1. There was variability, with resulting average values of Q_C' and P of 40 kJ /mole and 10.4 kCoul /mole respectively. As expected since only the cathodic behavior of the steel was being characterized, there was no clear above-the-scatter differentiation between results from steel in the slabs that contained C or W anodes. It is noted that the value of P that could be inferred from the apparent cathodic Tafel slope (βc~0.14V) at the temperatures of interest is in the order of ~40 kCoul/mole, much above the average in Table 1. Given the sweeping simplifications used in the above derivations, the values of P listed in Table 1 should then be viewed for now only as those of a convenient fit parameter. Trials where the value of P was forced to that estimated from βc yielded an overall fit quality that was not much degraded from that obtained with a fully adjustable P value, suggesting that the present data precision is not enough to resolve the issue. Neglecting the correction for potential altogether (setting P=0) created yet additional but minor degradation of the fit quality. Despite the overall uncertainty, the average value of Q_C' obtained by the procedure where P is treated as a fit parameter did fall in the order of apparent activation energies reported by others in comparable systems as shown in Table 2 [1, 4, 7, 9-11, 18] Moreover, application of the differential data processing approach with adjustable P served to significantly reduce the temperature-related scatter of the results and to develop better defined cathodic polarization curves for subsequent use in predictive models.[13,16] Notable examples are illustrated in Figure 3, where the upper graph shows E-log i diagrams constructed from the experimental results without temperature correction, while the lower graphs shows a marked reduction in scatter after temperature correction.

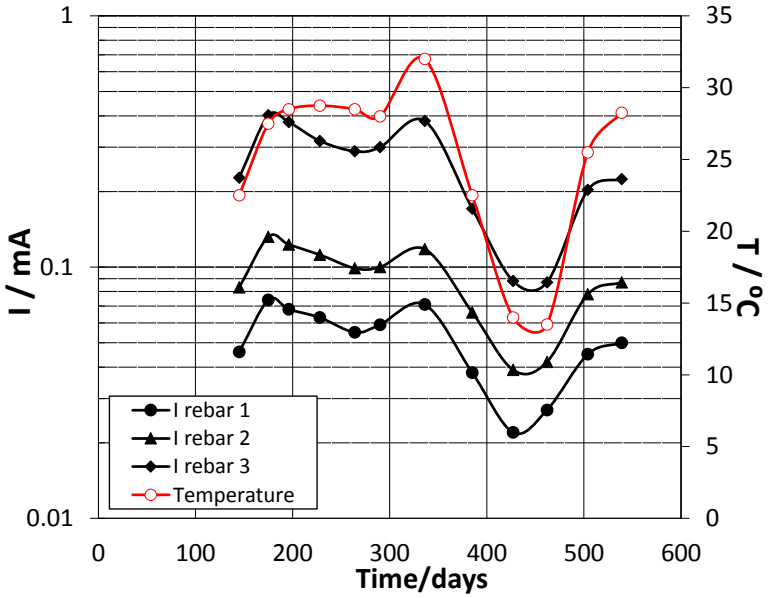

Figure 2: Example of current and temperature data for cathodic current from rebar # 1, 2 and 3 (Slab 1 - C anode).

Table 1
Calculated values of P and Q_C' for each Slab

Parameter	Slab 1 (C)	Slab 2 (W)	Slab 3 (C)	Slab 4 (W)	Slab 5 (C)	Slab 6 (W)
P (kCoul/mole)	7.20	10.48	15.09	14.75	-0.28	14.21
Q_C' (kJ/mole)	42.71	25.65	42.14	37.32	45.97	45.11

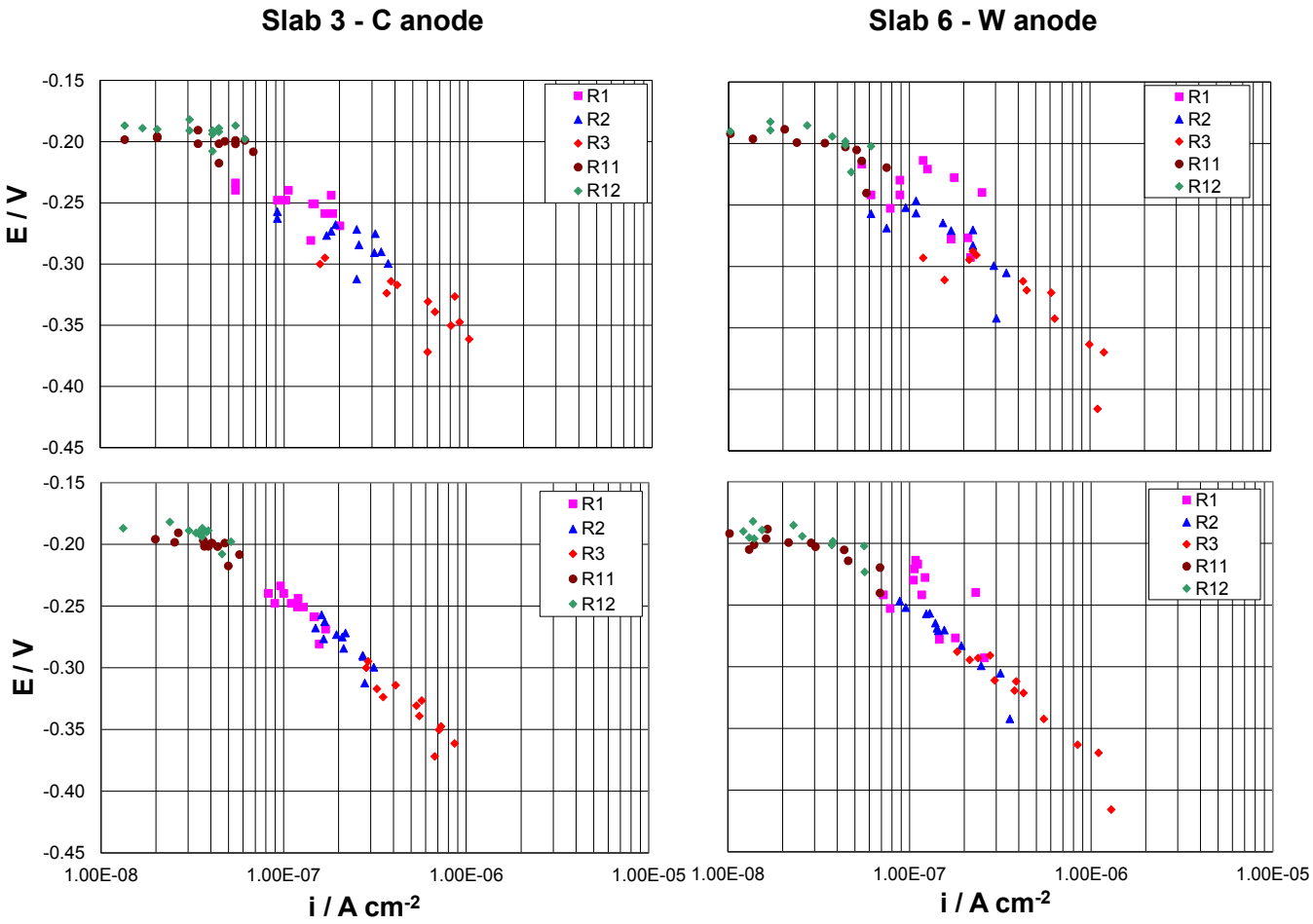

Figure 3: Examples of cathodic current density data from rebars # 1, 2, 3, 11, and 12. Top: Before temperature correction. Bottom: after correction using differential calculations.

Table 2
Activation energy values for cathodic current density -temperature dependence found by several authors.

Cathodic Current density	Activation Energy (kJ/mole)
Østvik. [7]	20.8 - 41.6
Jäggi et. al. [9]	35.8
Elsener et.al. [1]	31.5
Michael et.al. [11]	39
Raupach [10]	32
Lopez et. al. [18]	29 -33

Galvanic Current

Figure 4 (Top) illustrates the combined temperature and corrosion current evolution in a test slab showing how the galvanic current generally varied in strong correlation with short term and seasonal temperature changes, obscuring the long term analysis of anode aging trends. Comparable behavior was observed in companion slabs.

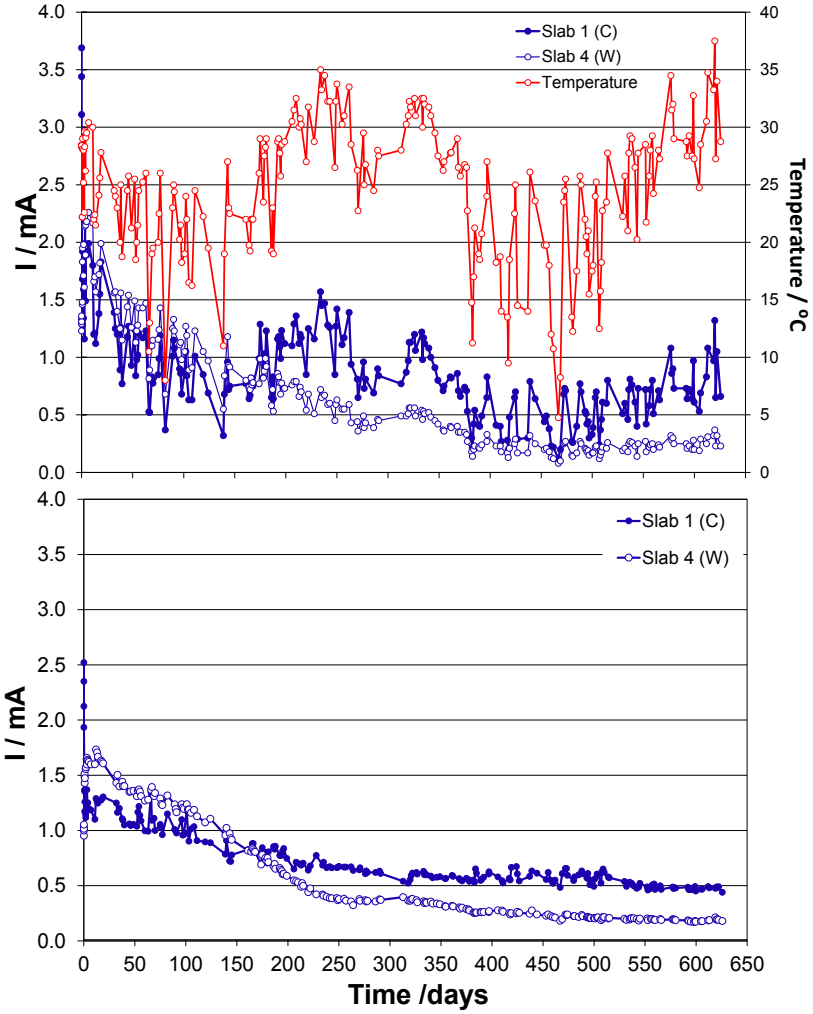

Figure 4: Top: Example of galvanic current and temperature data from Slab 1 (C anode) and 4 (W anode). Bottom: Trends for Slab 1 and 4 after correction using differential calculations.

The correlation between temperature and current was clearly established when plotting, consistent with Equation 9, R Δ (ln I) as function of Δ (T^{-1}), as exemplified in Figure 5 for data sets from Slab 1 (using the results from Figure 4, top) and from one of the slabs with a W anode. The slope of the well-defined fit lines (R^2>0.9) are the value of Q_A for the corresponding anode. Values of the entire slab set are shown in Table 3; average values were Q_A= 53 kJ/mole and 32 kJ/mole for the C and W anodes respectively, with relatively small variability within each anode type and establishing clear differentiation between both types. These values may be compared with activation energies in the order of ~30-40 kJ/mole for corrosion macrocell currents reported by other authors. [9-11, 18] Using Equation 9, the data sets for all the test slabs were corrected, with

results exemplified in Figure 4 (Bottom), where appreciable smoothing of the time trends can be observed. The corrected results were then successfully implemented in models for the projection of point anode behavior.[13]

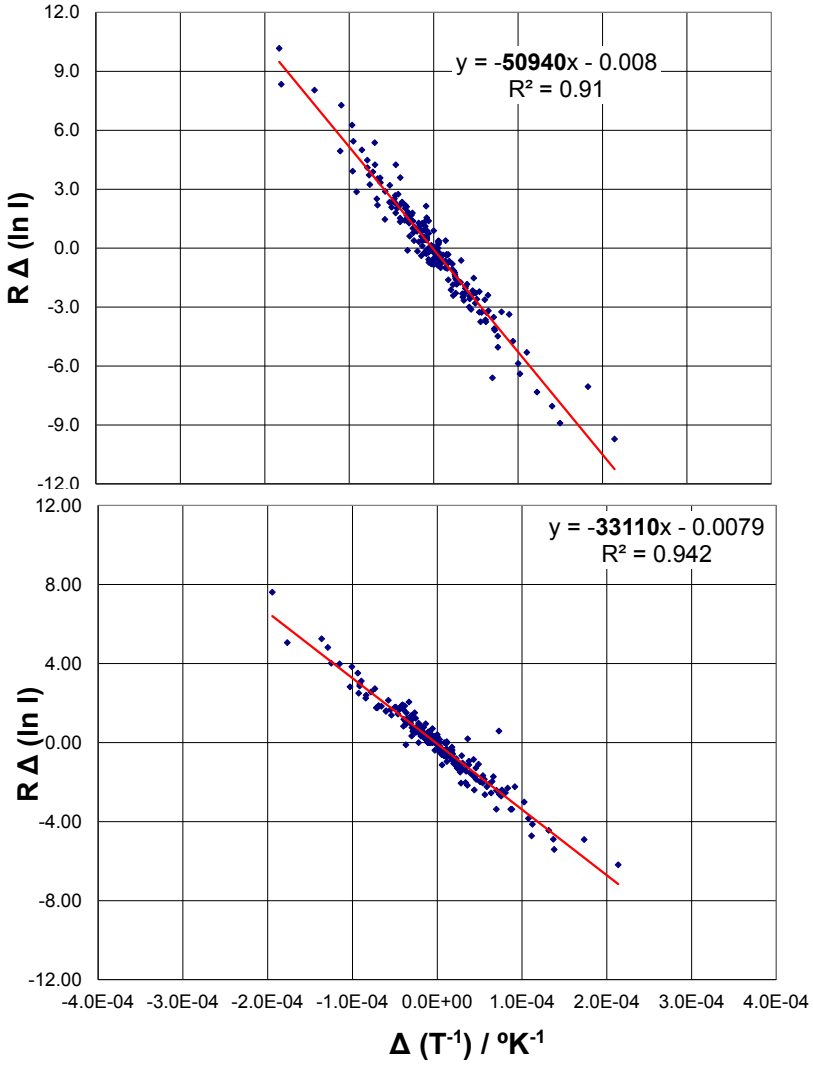

Figure 5: Examples of apparent activation energy calculation (slope of lines (kJ/mole) using differential calculations. Top: Slab 1, C anode. Bottom: Slab 4, W anode. I normalized to mA, R in J/(mole ºK).

Table 3
Calculated Activation Energy (kJ/mole) for each Anode Type

Activation Energy (kJ/ mole)			
C anodes		**W anodes**	
Slab 1	50.94	Slab 2	31.68
Slab 3	52.77	Slab 4	33.11
Slab 5	54.22	Slab 6	31.20
Average	52.64	**Average**	32.00

Electrical Resistivity of Concrete

Figure 6, Top illustrates an example for one of the test slabs of the combined resistivity and temperature data, showing the strong effect of temperature on concrete resistivity. The data were processed using the differential treatment and Equation 10 and setting T_r =298ºK.

As shown in Table 4, the resulting values of activation energy for the concrete in the chloride-free and chloride-laden zones were about the same (Q_R = 23-24 kJ/mole). Also as expected, the concrete resistivity was not a function of the anode type being evaluated since concrete makeup and chloride loading was the same in all slabs. A generic value of 24 kJ/mole was then used to process the entire data set as shown in Figure 6 (Bottom), where appreciable reduction of temperature-related scatter can be observed when comparing with the uncorrected data at the top. Activation energy values for concrete resistivity calculated in this study were in general agreement with those reported in the literature [5, 9, 17, 19-20], summarized in Table 5.

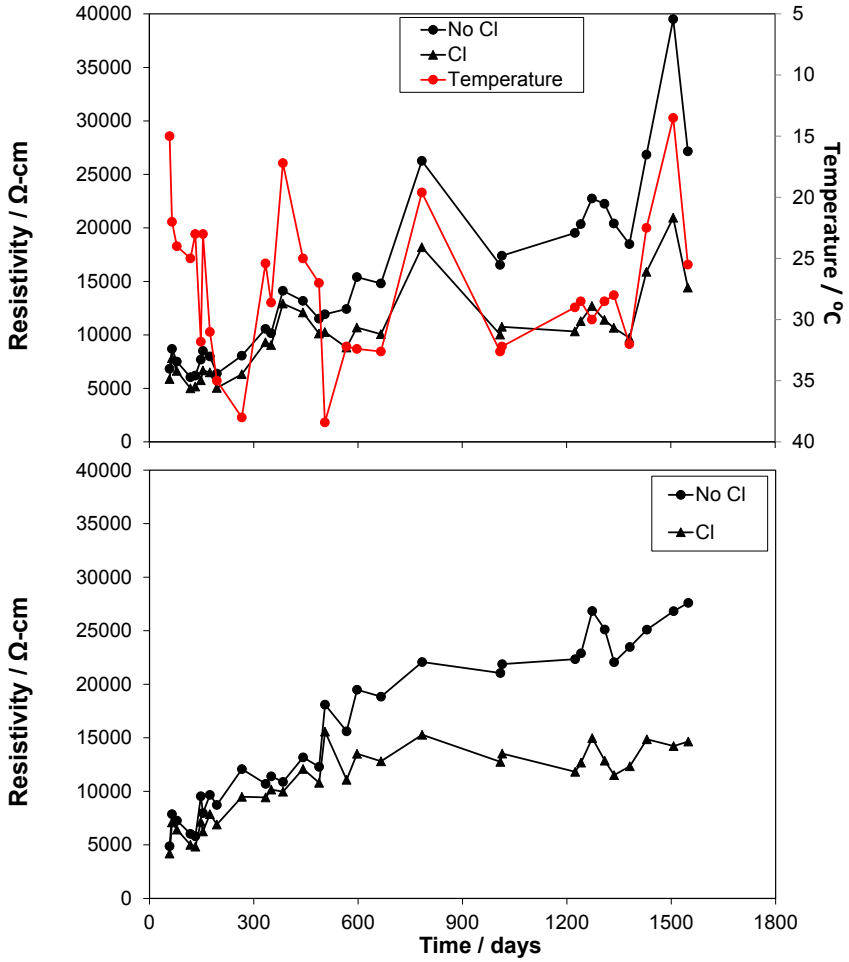

Figure 6: Example of Resistivity and temperature (inverted scale) data. Top: Average resistivity for chloride-free and chloride-laden zones. Bottom: Resistivity after correction using differential calculations.

Table 4
Calculated activation Energy (kJ/mole) for Resistivity

Activation Energy (kJ/ mole)		
	No Cl	**Cl**
Slab 1	23.44	22.54
Slab 3	24.86	26.73
Slab 5	23.42	20.37
Slab 2	25.38	26.03
Slab 4	22.15	22.17
Slab 6	24.45	23.06
Average	**23.95**	**23.48**

Table 5
Activation energy values for concrete resistivity temperature dependence found by several authors.

Resistivity	Activation Energy (kJ/mole)
Woelfl et.al. [19]	24.1
Hope et al. [20]	24
Virmani et. al. [17]	23.9
Jäggi et.al. [9]	25.6
Pour-Ghaz et.al. [5]	27

CONCLUSIONS

- Galvanic current and individual cathodic currents on passive steel in an outdoors reinforced concrete system with point anodes were markedly dependent on concrete temperature, introducing significant scatter in the system performance data and obscuring aging and polarization trends.

- Measured values were successfully standardized to an equivalent resistivity/current at a predefined reference temperature, through the application of a master temperature correction equation based on a differential formulation that derived correction parameters from short term fluctuations and filtered long term aging trends.

- A more refined steel cathodic polarization characterization was introduced and demonstrated by accounting for the effect of electrode potential, as an added term to the nominal activation energy of the cathodic reaction.

ACKNOWLEDGEMENTS

This investigation was supported by the State of Florida Department of Transportation and the U.S. Department of Transportation. The opinions, findings and conclusions expressed in this publication are those of the authors and not necessarily those of the supporting agencies.

REFERENCES

1. Elsener, B., “Corrosion rate of steel in concrete – Measurements beyond the Tafel law", CORROSION SCIENCE 47, (2005): pp. 3019-3033.
2. Chrisp, T., Starrs, G., McCarter W., Rouchotas, E., Blewett, J., “Temperature-conductivity relationships for concrete: An activation energy approach”, JOURNAL OF MATERIALS SCIENCE LETTERS 20, (2001): pp. 1085-1087.
3. Živica, V., Krajči, L’., Bágel’, L’. and Vargová, M., “Significance of the ambient temperature and the steel material in the process of concrete reinforcement corrosion”, CONSTRUCTION AND BUILDING MATERIALS, Vol. 11, No. 2, (1997): pp. 99-103.
4. Østvik, J-M., “Thermal aspects of corrosion of steel in concrete – PhD. Thesis”. The Norwegian University of Science and Technology, Department of Structural Engineering, (2004).
5. Pour-Ghaz, M., Burkan, O., Ghods. P., “The Effect of temperature on the corrosion of steel in concrete. Part 1: Simulated Polarization Resistance test and model development”. CORROSION SCIENCE 51, (2009): pp. 415-425.
6. Pour-Ghaz, M., Burkan, O., Ghods. P., “The effect of temperature on the corrosion of steel in concrete. Part 2: Model verification and parametric study”. CORROSION SCIENCE 51, (2009): pp. 426-433.
7. Østvik, J-M., Larsen, C.K., Vennesland, Ø., Sellevold, E.J., Andrade, M.C., “Electrical resistivity of concrete - Part I: Frequency dependence at various moisture contents and temperatures”, 2nd International RILEM[A] Symposium on Advances in Concrete through Science and Engineering, 2006.
8. Polder, R., “Test methods for on-site measurement of resistivity of concrete”, MATERIALS AND STRUCTURES, Vol. 33, (Dec 2000): pp 603-611.
9. Jägui, S., Böhni, H. and Elsener, B., “Macrocell corrosion of steel in concrete – Experiments and Numerical Modeling”, EUROCORR 2001 (Riva di Garda, ITALY).

[A] International Union of Laboratories and Experts in Construction Materials, Systems and Structures, 157 rue des Blains, F- 92220 Bagneux, FRANCE

10. Raupach, M. “Result from laboratory tests and evaluation of literature on the influence of temperature on reinforcement corrosion”, Corrosion of Reinforcement in Concrete-Monitoring, Prevention and Rehabilitation. pp. 9-20.

11. Michel, P.V.Nygaard, M.R.Geiker, “Experimental investigation on the short-term impact of temperature and moisture on reinforcement corrosion”, CORROSION SCIENCE 72 (2013) pp. 26–34

12. Dugarte, M.J and Sagüés, A.A., “Sacrificial Point Anodes for Cathodic Prevention of Reinforcing Steel In Concrete Repairs - Part 1: Polarization Behavior**”**. To appear in CORROSION, Volume 70, Issue 4 (2014).

13. Dugarte, M.J. and Sagüés, A.A., “Sacrificial Point Anodes for Cathodic Prevention of Reinforcing Steel in Concrete Repairs - Part 2: Performance Modeling**”**. To appear in CORROSION, Volume 70, Issue 4 (2014).

14. Kaesche H., “Corrosion of metals: physicochemical principles and current problems”. 1st ed. Berlin: Springer. (2003).

15. Tanaka, N., and Tamamushi, R., “Kinetic Parameters of Electrode reactions”. ELECTROCHIMICA ACTA, Vol. 9, (1964): pp.963-989.

16. Sagüés, A. A., Pech-Canul, M. A. and, Shahid Al-Mansur, A. K. M., “Corrosion Macrocell Behavior of Reinforcing Steel in Partially Submerged Concrete Columns”, CORROSION SCIENCE, Volume 45, (2003): p. 7

17. Virmani, Y.P., Clear, K.C., and Pasko, T.J.. 1983. Time-to-Corrosion of Reinforcing Steel in Concrete Slabs, Vol. 5, Calcium Nitrite Admixtures or Epoxy-Coated Reinforcing Bars as Corrosion Protection Systems. FHWA/RD83/012. Federal Highway Administration (FHWA)[B], Washington, D.C.

18. López, W., González, J.A., Andrade, C., “Influence of temperature on the service life of rebars”, CEM. CONCR. RES. 23 (1993):pp.1130–1140.

19. Woelfl, G.A. and Lauer, K., “The Electrical Resistivity of Concrete with Emphasis on the Use of Electrical Resistance for Measuring Moisture Content,” CEMENT, CONCRETE, AND AGGREGATES, CCAGDP, Vol. 1, No. 2, (1979): pp. 64-67.

20. Hope, B.B., Ip, A.K., and Manning, D.G., “Corrosion and Electrical Impedance in Concrete,” CEMENT AND CONCRETE RESEARCH, Vol. 15, No. 3, (1985): pp. 525-534.

[B] Federal Highway Administration (FHWA), 1200 New Jersey Ave., SE, Washington, DC 20590